Device-to-Device communication in an uplink channel for a 5G mm-Wave cellular network

Atul Sachan
National Institute of Technology Silchar
Subhra Sankha Sarma (subhra3s@gmail.com)
National Institute of Technology Silchar https://orcid.org/0000-0003-1826-0292
Ranjay Hazra
National Institute of Technology Silchar
FA Talukdar
National Institute of Technology Silchar

Research Article

Keywords: D2D communication, Power control, Coverage probability, Mode selection

Posted Date: June 24th, 2022

DOI: https://doi.org/10.21203/rs.3.rs-1780213/v1

Device-to-Device communication in an uplink channel for a 5G mm-Wave cellular network

Atul Sachan[1], Subhra Sankha Sarma[2*†], Ranjay Hazra[2†] and FA Talukdar[1†]

[1]Department of Electronics and Communication Engineering, NIT Silchar, Silchar, 788010, Assam, India.

[2]Department of Electronics and Instrumentation Engineering, NIT Silchar, Silchar, 788010, Assam, India.

*Corresponding author(s). E-mail(s): subhra3s@gmail.com;
Contributing authors:
atul_pg@ece.nits.ac.in; ranjayhazra87@gmail.com; fazal@ece.nits.ac.in;
†These authors contributed equally to this work.

Abstract

The exponentially growing need for higher data rates and the ubiquitous usage of smartphones has led to unprecedented issues in providing seamless communication while satisfying bandwidth constraints. Enabling Device-to-Device (D2D) communication in the millimeter-wave (mm-Wave) network enhances throughput and bandwidth but at the cost of higher pathloss attenuation. Also, D2D communication introduces interference in the traditional cellular network (CN), leading to degradation in the system performance. Thus, the proposed scheme applies dynamic mode selection criteria for efficient D2D communication in a 5G mm-Wave CN. The radius of coverage of D2D users (D2Ds) is derived for switching of the modes, i.e. from inner to outer. The outer mode switching occurs when the D2Ds suffer from extensive pathloss attenuation or with increase in coverage radius. Furthermore, power optimization is done to obtain optimal D2D transmit power thereby, enhancing the data rate, which is solved using the Lagrangian dual optimization technique. The performance metric, coverage probability is also derived which depicts the capability of the proposed scheme at a higher pathloss attenuation maintaining the Quality-of-Service (QoS) constraint. Simulation results prove the efficacy of the proposed scheme. Finally, the proposed scheme is compared with the state-of-the-art schemes which further proves the superiority of the proposed scheme in terms of better efficiency.

Keywords: D2D communication, Power control, Coverage probability, Mode selection

1 Introduction

A plethora of new applications, like smart grid, Internet of Things (IoT), and Internet of Vehicles (IoV), are expected to be supported under the umbrella of 5G systems. The proliferation of intelligent devices and the introduction of the latest multimedia applications, together with exponential growth in the demand and usage of wireless data, are already creating a burden on existing cellular networks. Remote control of appliances and electronic business machines over a dependable 5G network is expected to be available with minimal delay in a realistic "technological world". Mobile

users will control machines in real-time, making the IoT more accessible to everyone. Finally, but not least, less energy-intensive nodes in the network will be necessary to achieve an eco-friendly era. Agiwal et al. [1] present a comprehensive review of the transition of cellular networks from 1G to 5G. Mobile networks are likely to benefit from 5G in terms of data transmission speed, scalability, connection, and energy efficiency (EE).

In this modern era, D2D communication via cellular network (CN) is seen as a critical approach for mitigating the exponential increase of user expectation for extremely low latency, high data rate and low power consumption. The primary improvement in uplink performance is turning out to be progressively significant because of the increasing popularity of symmetric traffic applications like social networking, video calls, real-time generation and sharing of media content. D2D communication is a direct link between the two devices or users in close proximity that does not need a base station (BS) deployment. Nowadays, new applications, such as location-awareness and content distribution advertising, have resulted in several innovative D2D use cases in CN. D2D users (D2Ds) may share their data either in overlay or underlay mode. In overlay D2D communication, there is no overlap of resources between the cellular users (CUs) and D2Ds. However, because of the restricted usage of the authorized spectrum, overlay D2D depicts extremely low efficiency and throughput. In contrast, the underlay spectrum allows D2Ds to share bandwidth with CUs, enhancing the overall throughput and efficiency. The article [2-3] suggests that D2D communication via CN is still in its early phases, with power control and interference management challenges. Wei et al. [4] discusses some significant D2D communication technological problems and certain critical research factors that enable D2D communication in underlay CN. The topics covered are distance-based resource allocation, power control, mode selection and multi-antenna transmission techniques for D2D communication. Gupta and Jha [5] proposed a survey on 5G network and discussed short-range communication technologies such as mm-Wave communication, small cell, visible light communication (VLC), and WiFi, depicting increased data rate for inside users. Literature on 5G CN design, D2D communication, and machine-to-machine (M2M) connectivity is also highlighted. Uplink frequency is chosen to be lesser than downlink channel frequency in mobile communication because transmit power is more valuable at the battery end. Also, lower frequency suffers from lesser pathloss which helps in mitigating the interference [6]. Hence, uplink channel frequency is preferred over downlink frequency. Shah and Li [7] proposed a relay-assisted D2D communication, allowing devices to exchange data and extend the coverage through a relay technique for increased transmission distance and capacity. Using a commonly known analytical method, the effective capacity (EC), researchers assessed the statistical quality-of-service (QoS) guarantees of a D2D network assisted by a full-duplex (FD) relay. Bany and Haythem [8] proposed a protocol that uses D2D multi-hop transmission to reduce latency for individual downlink communication while maximizing network resource usage, leading to enhanced overall throughput. For single and multi-channel scenarios, the performance of the proposed protocol is compared to that of the IEEE 802.11a-based protocol. The severe interference at the cell edges is the most visible constraint that Ultra-Reliable Communication (URC) faces. To reduce interference and use URC, authors in [9] adopted Interference Management (IM) techniques like Soft Frequency Reuse (SFR) and Fractional Frequency Reuse (FFR).

Worldwide bandwidth constraint has encouraged research into adopting mm-Wave frequency spectrum for next-generation D2D communication networks and cellular broadband, posing issues for wireless operators. To enable D2D communication in the mm-Wave frequency, hurdles must be tackled and dealt with. The frequency and the wavelength range for the mm-Wave communication are 30-300 GHz and 1 to 10 mm, respectively. mm-Wave communication has the following characteristics: (*i*) more considerable propagation loss than the microwave band, (*ii*) smaller wavelength, and (*iii*) larger penetration loss. The smaller wavelength of the mm-Wave frequency causes problems in diffraction to the BS broadcast signal. Because the transmitted signal has a higher penetration loss than the microwave spectrum, it is primarily restricted to indoor conditions [10]. A frequent misconception in the wireless engineering industry is that rain and atmospheric

conditions render the mm-Wave spectrum unsuitable for mobile communication. Experimentation [10] shows that air absorption affects signal transmission for cell sizes of less than 200 m. At 28 GHz, a pathloss of 0.012 dB is observed for a cell size of less than 200 m. Similarly, for a distance above 200 m, a path loss of 1.4 dB is measured at 28 GHz. mm-Wave signal suffers considerable path loss as it travels through a concrete structure or solid material. Concrete walls and painted boards exhibit 178 dB and 20 dB attenuation at 40 GHz, respectively [10]. At the 5G mm-Wave network, interference is a major stumbling block for D2D communication in the 5G mm-Wave network. There are two forms of interference in D2D communication: co-channel and cross-channel interference. Cross-channel interference occurs when two users operating on distinct channels interfere with each other. Co-channel interference refers to interference between two users operating on the same frequency. Service providers can currently expand beyond the present 4G channel capacity of 20 MHz using the mm-Wave spectrum. The authors in [11] discussed resource allocation and frequency reuse approaches to overcome interference and efficiency issues, as well as proposed an experience based dynamic soft frequency reuse technique in the 28GHz 5G mm-Wave band. Users at the cell edge experience low throughput and signal-to-interference-plus-noise ratio (SINR). The proposed technique dynamically shares resources between cells and prevents unused resources from being wasted. The mode selection for D2D communication in a CN was explored in this research.

1.1 Related works

D2D mode switching is energy efficient as it decreases the usage of user terminal energy. Feng et al. [12] proposed a framework to address optimization challenges in each of the three transmission modalities. In dedicated and cellular modes, the author first uses the parametric Dinkelbach technique to divide the optimization issue into sequential convex subproblems. The optimization issue becomes more difficult while reusing the model owing to interference between the RCU (regular cellular users) and the D2D pair. The authors solved the problem by using concave-convex method (CCCP) subproblems after the parametric Dinkelbach transformation by repeatedly linearizing the non-convex component of the objective function [12]. Huang et al. [13] proposed that if a pair of D2Ds are in proximity and orthogonal resources are provided, framework adopts D2D dedicated mode. The proposed model combines mode selection, power control, and resource allocation into a unified framework. EE is utilized instead of sum rate as a goal, which is significant for uplink scenarios, while faulty channel state information (CSI) is another practical consideration. Khuntia et al. [14] proposed a resource sharing method for channel assignment and power allocation in a downlink scenario for D2D communication. A new approach is presented to increase the system capacity without interfering with the QoS of CUs. Several D2Ds utilize the same CUs channel, and each D2D pair reuses numerous channels from various CUs. Following channel assignment, power optimization is done on the pre-assigned channels for each D2D user using the Lagrangian dual optimization technique. This leads to the maximization of the sum rate of D2Ds. Chia-Hao et al. [15] demonstrated how interference between two links might be coordinated to improve the total rate without overpowered cellular service and proper power control. The work focuses on the optimal sum rate via power control for various modes. The author assumed a complete CSI scenario for the base station (BS) to optimize resource sharing mode selection. Lee et al. [16] proposed a centralized and distributed power control approach based on stochastic geometry for D2D underlay cellular systems. Because of the additional D2D connections, centralized power regulation improves the CN throughput while ensuring regular communication for uplink CUs. Future research might look at the impact of numerous BS antennas, other cell interferences, and optimization of combined resource allocation and power management. Venugopal et al. [17] discussed some important facts such as very high throughput (upto the order of Gbps) for D2D communication among wearable devices in mm-Wave frequency. Interference may be a major problem when a number of these devices are in close proximity. This study examines the performance of the mm-Wave network with a finite number of interferers in a finite network region using stochastic geometry. The preliminary results are that even with omnidirectional transceiver antennas,

mm-Wave frequencies may offer gigabit throughput, and system performance is improved with more directed antenna arrays. Sarma et al. [18] discussed the performance of D2D communication for an uplink channel in an underlay mm-Wave based network. The mm-Wave spectrum contributes considerable interference, resulting in pathloss attenuation of the user's signal. The suggested power control system offers a mechanism for ensuring maximum throughput by keeping the power within upper and lower boundaries. The suggested scheme's low outage probability assures higher performance, which undoubtedly allows D2D communication in the 5G mm-Wave network. This approach ultimately assures the system network's fairness. mm-Wave communication, which allows mobile devices to receive tremendously high data rates, is a promising technology for 5G CN. In order to exploit the massive bandwidth available on the directional mm-Wave network, D2D communication needs to be integrated. mm-Wave BSs can also be densely deployed in metropolitan areas to achieve optimal transmission rates and overall capacity. Fast neighbour discovery is necessary for mobile users to discover neighbouring BSs and switch to the BS with the best signal quality [19].

In mm-Wave based 5G networks, a promising interference management methodology for overlay D2D communication is proposed. For the problem elimination, the theory offers an alternative offer bargaining game (AOBG), which is a quasi Nash bargaining solution. D2Ds in close proximity strive for a higher SINR. The likelihood of an outage diminishes as the SINR level rises. The presented theory indicates that when distance and interference grow, the system throughput and SINR can be kept substantially constant [20]. Zhong et al. [21] proposed a scheme for potential coverage for both CUs and D2Ds. CUs rely on FD mode relays to connect to the BS. If the necessary SINR is less than 5dB, FD relay-assisted transmission can enhance D2D network. mm-Wave acts as a catalyst for next-generation cellular networks as a carrier frequency. Existing Ultra High Frequency (UHF) mobile network ideas are not well adapted to mm-Wave networks. The findings in [22] show that adding a relay node to the cellular or D2D network improves the coverage probability. Transmission capacity varies with node density for various SINR thresholds. Sarma et al. [23] discussed that D2D communication is advantageous at 28 GHz because 5G architecture facilitates enormous IoT connection leading to improvement in spectrum efficiency (SE). When data is sent from sensors to end-users over an IoT network, interference impacts the system. As a result, an effective resource allocation strategy is required to reduce interference while enhancing data flow. Dynamic sectorization is used to overcome the issues of user traffic. Following that, a power optimization issue is constructed and solved using the Lagrangian dual optimization approach. The summary of the related works portraying the objectives, optimization techniques and other parameters are shown in Table 1.

1.2 Contribution

The authors in the article focuses on the trade-off between the pathloss attenuation and dynamic mode selection for D2Ds in a 5G mm-Wave network employing an uplink channel. The main contribution of this paper is furnished as follows:

(a) Interference such as blockage effect, atmospheric attenuation, rain attenuation, foliage loss etc. is minimized using the proposed power optimization technique.

(b) Radius of coverage for communication between D2Ds is derived by switching the modes. D2Ds employ dynamic mode selection criteria based on the derived coverage radius. D2D communication is mostly accomplished via the inner mode. However, due to dense proximity users, increase in pathloss attenuation, and poor SINR, D2D communication is switched to outer mode.

(c) The proposed power optimization allocation problem is a non-convex mixed-integer non-linear programming (MINLP) problem that can not be solved in polynomial time. Using the Lagrangian dual optimization approach, the optimal power for each D2Ds is calculated from the predetermined channels.

(d) Further, the performance of the system is analyzed by deriving the coverage probability of D2Ds for varying pathloss exponents.

(e) The proposed scheme is also compared with the state-of-the-art technique which proves its efficiency over the state-of-the-art schemes.

The remainder of this article is categorized as follows. In Section 2, the system and path loss model with some basic assumptions are discussed. Section 3 presents the problem formulation for dynamic mode selection of D2D communication employing an uplink channel in a 5G mm-Wave network. Further, the mathematical analysis of coverage radius, power optimization and coverage probability of D2Ds in inner and outer modes is presented. In Section 4, simulation results and the analysis of results are presented, followed by the conclusion and future work in Section 5.

2 Proposed scheme

2.1 System model

A single cell is considered in a 5G mm-Wave based uplink CN with numerous CUs, D2Ds, and their interferences on D2Ds as shown in Figure 1. In our work, we have considered an uplink channel because it showcases lesser interference than the downlink channel [24]. The BS is placed at the focal point of the cell. In this scenario, a total of N number of CUs keyed by $C = [1, 2, ...N]$ and L number of D2Ds keyed by $D = [1, 2, ...L]$ are unevenly distributed in the same cell ensuing Poison Point Process (P) (ϕ). Here, D2D communication is typically carried out in two modes namely, inner mode and outer mode. Inner and outer modes are defined by the value of the distance of the transmitter D2Ds from the BS, given by $r^{'}$. D2D communication is typically carried out in the inner mode, but with the increase in the number of proximate D2D devices and radius of coverage, communication gets switched to the outer mode. The proposed work considers that the uplink resource of a single CU can only be used by a single D2D at any particular time instant. The CUs and inner mode D2Ds use the cellular frequency, i.e., 2 GHz, while the outer mode D2Ds use the mm-Wave frequency, i.e., 28 GHz. It is assumed that the total number of channels is the same as the total number of CUs. Furthermore, it is also assumed that the BS has complete knowledge about the location of CUs and D2Ds, as well as their respective pathloss exponents. In addition, the BS is believed to have a comprehensive awareness of the CSI. The symbols and explanations used throughout the paper, as well as their definitions, are listed in Table 2.

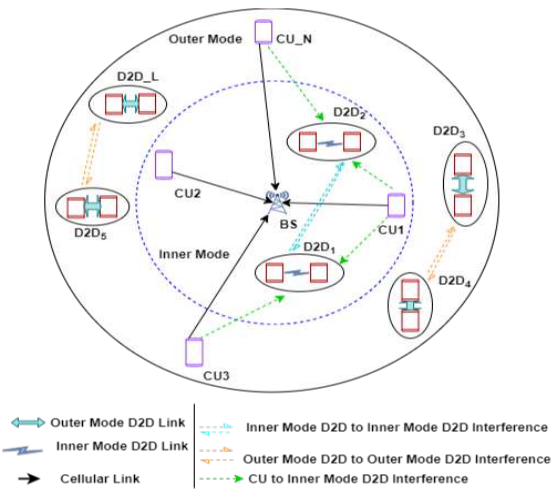

Fig. 1 System model portraying interferences on D2D users

2.2 Pathloss model

Communication in the mm-Wave spectrum encounters interference from various sources, as already mentioned. As a result, to limit the various interference, a stringent path loss model should be adopted. The path loss model used for free-space path loss (FSPL) is derived from [25] and is as follows,

$$FSPL(f, 1m)[dB] = 20\log_{10}\frac{(4\pi f_c \times 10^9)}{c} = 32.4[dB] + 20\log_{10} f_c \quad (1)$$

The carrier frequency is denoted by f_c, while the speed of light is denoted by c. In this paper, f_c is changed in accordance with the inner and outer modes. Inner mode D2D communication uses a frequency of 2 GHz, whereas outer mode D2D communication occurs at a frequency of 28 GHz. The pathloss in dB for free space at a transmitter-receiver (T-R) distance of 1m is represented by $FSPL(f, 1m)$. Nowadays, many buildings possess infrared reflective glasses, and the penetration loss correlated with them varies. As a result, the large scale pathloss model as defined by NYUSIM [25] for a 1 m reference distance is as follows,

$$PL(f, d)[dB] = FSPL(f, 1m)[dB] + 10\alpha\log_{10}(d) + AT[dB] + \chi_\sigma \quad (2)$$

Table 1 List of notations

Symbols and their significance		
S.No	Symbols	Definitions
1	N	Number of CUs
2	L	Number of D2Ds
3	f_c	Carrier frequency
4	d	Distance between T-R
5	σ	Standard deviation in decibel
6	α	Path loss exponent of the channel
7	β	Power compensation factor
8	A_a	Interference due to atmospheric absorption
9	P_x, P_y, P_k, P_z	Transmit power of x^{th} CU user, y^{th} D2D inner mode user, k^{th} D2D outer mode user and z^{th} rest of the users
10	G_x, G_y, G_k, G_z	Rician channel coefficients for cellular links, inner mode D2D, outer mode D2D and the remainder of the users
11	d_x, d_y, d_k	Distance across CUs, inner mode D2Ds, and outer mode D2Ds
12	Y_c, Y_{d_i}, Y_{d_o}	Signal received by CUs, inner mode D2Ds, and outer mode D2Ds
13	$\gamma_c, \gamma_{d_i}, \gamma_{d_o}$	SINR for cellular, inner mode D2Ds as well as outer mode D2Ds
14	$P_{x_{max}}$	Maximum tolerable interference which the D2Ds can persist
15	R_c, R_{d_i}, R_{d_o}	Total sum rate associated with CU, inner mode D2D and outer mode D2D
16	ϕ	Poisson Point Process Distribution
17	γ_{th}	Minimum SINR Threshold
18	B_1, B_2	Bandwidth allocated to inner and outer modes
19	r	Coverage radius
20	ρ_c, ρ_{d_i}	Density of CUs as well as inner mode D2Ds
21	λ, μ	Lagrangian multipliers
22	δ	Weight parameter for controlling transmit power
23	Q_p	Set containing all the transmission powers for D2Ds
24	I_c, I_{d_i}	Interference at cellular and inner mode D2Ds
25	$\mathcal{L}_{I_c}(s), \mathcal{L}_{I_{d_i}}(s)$	Laplace transform of interference at CUs and D2Ds
26	P_{max}	Total transmit power budget of the user
27	σ_n^2	Thermal noise power
28	η	Shadow fading with a log-normal distribution and zero mean
29	N_o	Thermal noise component

where d represents the three-dimensional separation distance between the T and R, α the path loss exponent, χ_σ denotes the log normal shadow fading having zero mean with σ standard deviation (in dB), and AT the atmospheric absorption interference.

The channel gain (Rician fading channel) G between two users may be expressed as $G = 10^{(\frac{-PL}{10})}$, which is proportional to the distance between T and R and has an independently and symmetrically exponential distribution with a mean of μ^{-1}. The existence of a stronger line of sight signal component when the amplitude gain is defined by Rician distribution is termed a Rician fading channel [26].

3 Problem formulation

The expression for the received power of CUs and D2Ds following Rician distribution is as follows,

$$P_r = P_t.G.d^{\alpha(\beta-1)};\ P_t \in (0, P_{max}) \tag{3}$$

where P_t represents the transmitted power, and β denotes the power compensation factor. If $\beta = 0$, no power compensation is applied to the signal path loss. When $\beta = 1$, it means that path loss has been entirely compensated.
When the CU communicates with the BS, the received signal comprising of the interference from the other CUs as well as some of the other D2Ds, can be depicted as follows,

$$Y_c = \sqrt{P_x.G_x.{d_x}^{\alpha(\beta-1)}} + \sum_{y=1}^{L} \sqrt{P_y.G_y.{d_y}^{\alpha(\beta-1)}} + \sum_{\substack{z=1 \\ z\neq x}}^{M} \sqrt{P_z.G_z.{d_z}^{\alpha(\beta-1)}} + N_o \tag{4}$$

The first term in this equation reflects the signal received from the BS. The second term represents the sum of all those interference coming from different users. The third component is the sum of all D2D user interference, while the last term represents the thermal noise component (N_o). In this case, the distribution of the CUs and D2Ds is represented by PPP i.e. ϕ.
Similarly, the signal received by the D2D user in the inner mode is as follows,

$$Y_{d_i} = \sqrt{P_y.G_y.{d_y}^{\alpha(\beta-1)}} + \sum_{x=1}^{M} \sqrt{P_x.G_x.{d_x}^{\alpha(\beta-1)}} + \sum_{\substack{z=1 \\ z\neq y}}^{L} \sqrt{P_z.G_z.{d_z}^{\alpha(\beta-1)}} + N_o \tag{5}$$

In this case, P_x and P_y indicate the transmission power of the x^{th} CUs and the y^{th} D2Ds in inner mode, respectively. The distance between a pair of D2Ds in inner mode and a pair of CUs is represented by d_x and d_y respectively. The Rician channel fading coefficients of cellular link and inner mode D2D link is indicated by G_x and G_y respectively.
Similarly, the signal received by the D2Ds in the outer mode is as follows,

$$Y_{d_o} = \sqrt{P_k.G_k.{d_k}^{\alpha(\beta-1)}} + \sum_{\substack{z=1 \\ z\neq k}}^{L} \sqrt{P_z.G_z.{d_z}^{\alpha(\beta-1)}} + N_o \tag{6}$$

In this case, P_k represents the transmission power of the k^{th} D2D user in outer mode, whereas P_z indicates the transmission power of the remaining users, i.e., CU or D2D user. The distance between a pair of D2D user in outer mode is denoted by d_k. The Rician fading channel coefficients for the outer mode D2D link and the remainder of the users, i.e., CUs or D2Ds, respectively, are denoted by G_k and G_z respectively. Therefore, the SINR for CU can be expressed as,

$$\gamma_c = \frac{P_x.G_x.{d_x}^{\alpha(\beta-1)}}{\sum_{y=1}^{L} P_y.G_y.{d_y}^{\alpha(\beta-1)} + \sum_{\substack{z=1 \\ z\neq x}}^{M} P_z.G_z.{d_z}^{\alpha(\beta-1)} + \sigma_n^2} \tag{7}$$

Similarly, the SINR for the D2Ds in inner mode is given as,

$$\gamma_{d_i} = \frac{P_y.G_y.{d_y}^{\alpha(\beta-1)}}{\underbrace{\sum_{x=1}^{M} P_x.G_x.{d_x}^{\alpha(\beta-1)} + \sum_{\substack{z=1 \\ z\neq y}}^{L} P_z.G_z.{d_z}^{\alpha(\beta-1)} + \sigma_n^2}_{\mathrm{T}_c}} = \frac{P_y.G_y.{d_y}^{\alpha(\beta-1)}}{T_c} \tag{8}$$

And, the SINR for a D2Ds in outer mode is expressed as,

$$\gamma_{d_o} = \frac{P_k.G_k.{d_k}^{\alpha(\beta-1)}}{\sum_{\substack{z=1 \\ z\neq k}}^{L} P_z.G_z.{d_z}^{\alpha(\beta-1)} + \sigma_n^2} \tag{9}$$

Now, using Shannon's formula, the total sum rate for the CUs, and the D2Ds (for inner as well as outer modes) can be expressed as follows,

$$R_c = B_1 \log_2(1 + \gamma_c) \tag{10}$$

$$R_{d_i} = B_2 \log_2(1 + \gamma_{d_i}) \tag{11}$$

$$R_{d_o} = B_2 \log_2(1 + \gamma_{d_o}) \tag{12}$$

Here, B_1 and B_2 represents the bandwidth for CUs and D2Ds respectively.

3.1 Radius of Coverage

We have assumed that the SINR of inner mode D2Ds should be greater than or equal to the SINR threshold which can be written as follows,

$$\gamma_{d_i} \geq \gamma_{th} \tag{13}$$

Let us assume that $P_{x_{max}}$ be the maximum tolerable interference that the D2Ds can withstand, as obtained from equation (8). It is also assumed that $P_x = P_{x_{max}}$. Thus, from equation (8) the value for T_c can be expressed as follows,

$$\begin{aligned} T_c = &\sum_{x=1}^{M} P_{x_{max}}.G_x.{d_x}^{\alpha(\beta-1)} \\ &+ \sum_{\substack{z=1 \\ z\neq y}}^{L} P_z.G_z.{d_z}^{\alpha(\beta-1)} + \sigma_n^2 \end{aligned} \tag{14}$$

Now, we combine equations (13) and (14). We have assumed that $d_y = r$ which represents the distance of D2D transmitter from the BS,

$$\begin{aligned} \frac{P_y.G_y.r^{\alpha(\beta-1)}}{T_c} &\geq \gamma_{th} \\ r^{\alpha(\beta-1)} &\geq \frac{\gamma_{th}.T_c}{P_y.G_y} \\ r^{\alpha(1-\beta)} &\geq \frac{P_y.G_y}{\gamma_{th}.T_c} \end{aligned} \tag{15}$$

$$r \geq \left(\frac{P_y.G_y}{\gamma_{th}.T_c}\right)^{\frac{1}{\alpha(1-\beta)}} \rightarrow \text{for outer mode D2D} \tag{16}$$

$$r < \left(\frac{P_y.G_y}{\gamma_{th}.T_c}\right)^{\frac{1}{\alpha(1-\beta)}} \rightarrow \text{for inner mode D2D} \tag{17}$$

To communicate in inner mode, i.e. using cellular frequency, D2Ds must meet the conditions specified in equations (16) and (17). However, if the value of radius r surpasses the value $r^{'}$, the D2D is assigned to outer mode for communication where $r^{'} = \left(\frac{P_y.G_y}{\gamma_{th}.T_c}\right)^{\frac{1}{\alpha(1-\beta)}}$.

Therefore, equations (16) and (17) can serve as a criteria for dynamic mode selection for the D2Ds i.e. from inner mode to outer mode. The next subsection discusses about the power optimization scheme and also helps in the formulation of the problem statement for optimization.

3.2 Power Optimization

For every admissible D2D pair, the optimal power allocation for D2D pairs in inner and outer modes are considered to ba a maximization problem for a given QoS as shown below,

$$\max_{P_y \in Q_p} \left(\left(R_{d_i} + R_{d_o} \right) - \delta P_y \right) \tag{18}$$

subject to the constraints,

$$a1 : P_y \leq P_{max} \tag{19}$$

$$a2 : \frac{P_y.G_y.{d_y}^{\alpha(\beta-1)}}{T_c} \geq \gamma_{th};\ \beta \in (0,1) \tag{20}$$

The goal of the function is to maximize the D2D sum rate by taking into account the transmit power with some fixed weight $\delta(0, \infty)$, in order to increase the coverage capacity by reducing the necessary sum power. In this case, Q_p is the set that contains all of the transmission power for D2Ds. The limitation in equation (19) reflects the maximum power limit of each D2Ds, whereas the constraint in equation (20) represents the minimum threshold of D2D user in inner mode.

Here, β, a binary assignment variable $\beta(0, 1)$ signifies a power compensation factor. When the value of $\beta = 0$, there is no power compensation on the signal path loss, but if $\beta = 1$, it signifies that path loss is fully compensated. The best solution for the stated issue in equation (18) is difficult since the problem is non-convex because the objective function and restrictions are not jointly concave. The non-convex nature of the problem is optimised using Lagrange dual optimization in order to obtain an optimal solution.

The Lagrangian associated with the problem (18)

may be as follows,

$$
\begin{aligned}
&L(P_y, \mu, \lambda) \\
&= \delta P_y - B_2 \Bigg\{ \log_2 \left(1 + \frac{P_y G_y {d_y}^{\alpha(\beta-1)}}{T_c} \right) \\
&+ \log_2 \left(1 + \frac{P_k G_k {d_k}^{\alpha(\beta-1)}}{\sum_{\substack{z=1 \\ z \neq k}}^{L} P_z G_z {d_z}^{\alpha(\beta-1)} + \sigma_n^2} \right) \Bigg\} \\
&+ \lambda(P_y - P_{max}) + \mu \left(T_c - \frac{P_y G_y {d_y}^{\alpha(\beta-1)}}{\gamma_{th}} \right) \\
&= \delta P_y - B_2 \Bigg\{ \frac{1}{\ln 2} \ln \left(1 + \frac{P_y G_y {d_y}^{\alpha(\beta-1)}}{T_c} \right) \\
&+ \frac{1}{\ln 2} \ln \left(1 + \frac{P_k G_k {d_k}^{\alpha(\beta-1)}}{\sum_{\substack{z=1 \\ z \neq k}}^{L} P_z G_z {d_z}^{\alpha(\beta-1)} + \sigma_n^2} \right) \Bigg\} \\
&+ \lambda(P_y - P_{max}) + \mu \left(T_c - \frac{P_y G_y {d_y}^{\alpha(\beta-1)}}{\gamma_{th}} \right) \\
&= P_y \left[\delta + \lambda - \mu \left(\frac{G_y {d_y}^{\alpha(\beta-1)}}{\gamma_{th}} \right) \right] \\
&- \frac{B_2}{\ln 2} \ln \left[1 + \frac{P_y G_y {d_y}^{\alpha(\beta-1)}}{T_c} \right] - _{max} + _c \\
&- \frac{B_2}{\ln 2} \ln \left[1 + \frac{P_k G_k {d_k}^{\alpha(\beta-1)}}{\sum_{\substack{z=1 \\ z \neq k}}^{L} P_z G_z {d_z}^{\alpha(\beta-1)} + \sigma_n^2} \right]
\end{aligned} \tag{21}
$$

Let us assume that $\zeta = \delta + \lambda - \mu \left(\frac{G_y . {d_y}^{\alpha(\beta-1)}}{\gamma_{th}} \right)$. Now, differentiating equation (21) w.r.t P_y, we obtain,

$$
\begin{aligned}
&\frac{\partial L(P_y, \lambda, \mu)}{\partial P_y} \\
&= \zeta - \frac{B_2}{\ln 2} . \frac{1}{\left(1 + \frac{P_y . G_y . {d_y}^{\alpha(\beta-1)}}{T_c} \right)} . \frac{G_y . {d_y}^{\alpha(\beta-1)}}{T_c} \\
&= \zeta - \frac{B_2}{\ln 2} . \left(\frac{G_y . {d_y}^{\alpha(\beta-1)}}{T_c + P_y . G_y . {d_y}^{\alpha(\beta-1)}} \right)
\end{aligned} \tag{22}
$$

Now, equating equation (22) to zero, we get,

$$
\begin{aligned}
&\zeta = \frac{B_2}{\ln 2} . \left(\frac{G_y . {d_y}^{\alpha(\beta-1)}}{T_c + P_y . G_y . {d_y}^{\alpha(\beta-1)}} \right) \\
&\implies T_c + P_y . G_y . {d_y}^{\alpha(\beta-1)} = \frac{B_2}{\zeta \ln 2} . G_y . {d_y}^{\alpha(\beta-1)} \\
&\implies P_y . G_y . {d_y}^{\alpha(\beta-1)} = \frac{B_2}{\zeta \ln 2} . G_y . {d_y}^{\alpha(\beta-1)} - T_c \\
&\implies P_y = \frac{B_2}{\zeta \ln 2} - \frac{T_c}{G_y . {d_y}^{\alpha(\beta-1)}}
\end{aligned} \tag{23}
$$

To determine dual function $f(\lambda, \mu)$, we have replaced P_y in equation (23).

$$
\begin{aligned}
& f(\lambda, \mu) \\
& = \left[\frac{B_2}{\zeta \ln 2} - \frac{T_c}{G_y.{d_y}^{\alpha(\beta-1)}}\right]\zeta \\
& - \frac{B_2}{\ln 2}.\ln\left[1 + \frac{P_k.G_k.{d_k}^{\alpha(\beta-1)}}{\sum_{\substack{z=1 \\ z\neq k}}^{L} P_z.G_z.{d_z}^{\alpha(\beta-1)}}\right. \\
& \left. + \sigma_n^2\right] - \lambda.P_{max} + \mu.T_c\frac{B_2}{\ln 2}\ln\left[1\right. \\
& \left. + \frac{\left[\frac{B_2}{\zeta \ln 2} - \frac{T_c}{G_y.{d_y}^{\alpha(\beta-1)}}\right].\left(G_y.{d_y}^{\alpha(\beta-1)}\right)}{T_c}\right] \\
& = -\left[\frac{B_2}{\zeta \ln 2} - \frac{T_c}{G_y.{d_y}^{\alpha(\beta-1)}}\right].(-\zeta) \\
& - \frac{B_2}{\ln 2}.\ln\left[1 + \frac{P_k.G_k.{d_k}^{\alpha(\beta-1)}}{\sum_{\substack{z=1 \\ z\neq k}}^{L} P_z.G_z.{d_z}^{\alpha(\beta-1)}}\right. \\
& \left. + \sigma_n^2\right] - \lambda.P_{max} + \mu.T_c - \frac{B_2}{\ln 2}\ln\left[1\right. \\
& \left. + \left(\frac{1}{\zeta}\right).\frac{B_2.G_y.{d_y}^{\alpha(\beta-1)}}{(\ln 2).T_c} - 1\right] \\
& = \frac{B_2}{\ln 2}.\ln(\zeta) - \frac{T_c}{G_y.{d_y}^{\alpha(\beta-1)}}.(\zeta) \\
& - \frac{B_2}{\ln 2}.\ln\left[1 + \frac{P_k.G_k.{d_k}^{\alpha(\beta-1)}}{\sum_{\substack{z=1 \\ z\neq k}}^{L} P_z.G_z.{d_z}^{\alpha(\beta-1)} + \sigma_n^2}\right] \\
& - \lambda.P_{max} + \mu.T_c + \frac{B_2}{\ln 2}\ln\left[\frac{\ln 2}{B_2}\right. \\
& \left.\left(\frac{T_c}{G_y.{d_y}^{\alpha(\beta-1)}}\right)\right]
\end{aligned}
\tag{24}
$$

Let us assume,

$$
\begin{aligned}
\omega & = \frac{B_2}{\ln 2}\ln\left[\frac{\ln 2}{B_2}\left(\frac{T_c}{G_y{d_y}^{\alpha(\beta-1)}}\right)\right] \\
& - \frac{B_2}{\ln 2}\ln\left[1 + \frac{P_k G_k {d_k}^{\alpha(\beta-1)}}{\sum_{\substack{z=1 \\ z\neq k}}^{L} P_z G_z {d_z}^{\alpha(\beta-1)} + \sigma_n^2}\right] \\
& = \frac{B_2}{\ln 2}\ln\left(\delta + \lambda - \mu\left(\frac{G_y{d_y}^{\alpha(\beta-1)}}{\gamma_{th}}\right)\right) \\
& - \frac{T_c}{G_y{d_y}^{\alpha(\beta-1)}}\left(\delta + \lambda - \mu\left(\frac{G_y{d_y}^{\alpha(\beta-1)}}{\gamma_{th}}\right)\right) \\
& - _{max} + \mu T_c + \omega
\end{aligned}
\tag{25}
$$

As a result, the dual optimization problem is expressed as follows,

$$
min f(\lambda, \mu) \tag{26}
$$

subject to constraint,
$a3$: $\lambda, \mu \geq 0$.
Taking the gradient of f with respect to λ, μ and equating it to zero, yields the solution for λ, μ.

$$
\begin{aligned}
\bigtriangledown f(\lambda, \mu)\mid_{\lambda} = & \frac{B_2}{\ln 2}\frac{1}{(\delta + \lambda - \mu(\frac{G_y{d_y}^{\alpha(\beta-1)}}{\gamma_{th}}))} \\
& - \frac{T_c}{G_y{d_y}^{\alpha(\beta-1)}} - P_{max}
\end{aligned}
\tag{27}
$$

$$
\begin{aligned}
\bigtriangledown f(\lambda, \mu)\mid_{\mu} = & \frac{B_2}{\ln 2}\frac{1}{(\delta + \lambda - \mu(\frac{G_y{d_y}^{\alpha(\beta-1)}}{\gamma_{th}}))} \\
& \times (\frac{G_y{d_y}^{\alpha(\beta-1)}}{\gamma_{th}}) - \frac{T_c}{\gamma_{th}} + T_c
\end{aligned}
\tag{28}
$$

Updating the dual variable in the gradient direction yields,

$$
\lambda^{current} = \lambda^{previous} + \psi_1.\nabla f(\lambda, \mu)
$$

$$
\mu^{current} = \mu^{previous} + \psi_2.\nabla f(\lambda, \mu)
$$

where ψ_1 and ψ_2 are the minimum gradients used to compute the Lagrange factors.
KKT conditions are used to identify the optimum solution with zero duality. We assume that the solution to the primal and dual optimization problem is ${P_y}^*$, λ^* and μ^* respectively.

The required KKT conditions are furnished as follows,

$$L(P_y^*, \mu^*, \lambda^*) = \delta - \frac{B_2}{\ln 2} \frac{G_y.{d_y}^{\alpha(\beta-1)}}{\left(T_c + P_y^*.G_y.{d_y}^{\alpha(\beta-1)}\right)} + \mu^* \left(T_c - \frac{G_y.{d_y}^{\alpha(\beta-1)}}{\gamma_{th}}\right) + \lambda^* \tag{31}$$

$$\lambda^* \left[\left(P_y^* - P_{max}\right) = 0\right] \tag{32}$$

$$\mu^* \left[\left(T_c - \frac{P_y^* G_y.{d_y}^{\alpha(\beta-1)}}{\gamma_{th}}\right) = 0\right] \tag{33}$$

$$\left(P_y^* - P_{max}\right) \leq 0 \tag{34}$$

$$\left(T_c - \frac{P_y^* G_y.{d_y}^{\alpha(\beta-1)}}{\gamma_{th}}\right) \leq 0 \tag{35}$$

$$\lambda^* \geq 0 \tag{36}$$

$$\mu^* \geq 0 \tag{37}$$

Using the given KKT criteria, the best power solution obtained is given below,

$$P_y^* = \frac{B_2}{\ln 2\left[\delta + \lambda^* - \mu^*\left(\frac{G_y.{d_y}^{\alpha(\beta-1)}}{\gamma_{th}}\right)\right]} - \frac{T_c}{G_y.{d_y}^{\alpha(\beta-1)}} \tag{38}$$

The optimal power P_y^* for a given value of δ may be found by calculating the optimal λ^*, μ^*, and then replacing it in equation (38). The above expression (38) gives us the value for the optimized D2D transmit power in outer mode. The algorithm for allocation of resources to the available D2Ds is shown in Algorithm 1.

3.3 Coverage Probability of D2D Users

This section covers the probability of coverage for inner mode and outer mode D2Ds. It is noted that for interference limited environment, thermal noise power is zero i.e. ($\sigma_n^2 = 0$).

Algorithm 1 Allocation of resources to D2D pairs in different modes

```
Input : The set of D2D pairs and CU pairs are indexed by D_L and C_N.
Output: Interference minimization and transmit power optimization.
Initializing the number of D2D and CU pairs.
for N > L do
    for n = 1 : N do
        for l = 1 : (L − 1) do
            Calculate γ_{d_i}, γ_{d_o}, γ_c from (7-9)
            if γ_{d_i} ≥ γ_th
            r < r' then
                Allocation to inner mode
            else
                Allocation to outer mode
                a1, a2 & a3 are satisfied
                Update β, δ, λ & μ.
                Update P_y^* from equation (38).
            end if
            Increment of n and δ.
            Repeat
        end for
    end for
end for
```

$$\gamma_{d_i} = \frac{P_y.G_y.{d_y}^{\alpha(\beta-1)}}{\sum_{x=1}^{M} P_x.G_x.{d_x}^{\alpha(\beta-1)} + \sum_{\substack{z=1 \\ z\neq y}}^{L} P_z.G_z.{d_z}^{\alpha(\beta-1)}} \tag{39}$$

$$\gamma_{d_o} = \frac{P_k.G_k.{d_k}^{\alpha(\beta-1)}}{\sum_{\substack{z=1 \\ z\neq k}}^{L} P_z.G_z.{d_z}^{\alpha(\beta-1)}} \tag{40}$$

The coverage probability may be stated as the complementary cumulative distribution function (CCDF) of the SINR, which may be represented as a probability distribution function as shown

below,

$$
\begin{aligned}
P_{cov}^{d} &= \mathcal{P}[\gamma_{d_i} \geq \gamma_{th}] \\
&= 1 - \mathcal{P}[\gamma_{d_i} \leq \gamma_{th}] \\
&= 1 - \mathcal{P}\left[\frac{P_y.G_y.{d_y}^{\alpha(\beta-1)}}{\sum_{x=1}^{M} P_x.G_x.{d_x}^{\alpha(\beta-1)} + \sum_{\substack{z=1 \\ z\neq y}}^{L} P_z.G_z.{d_z}^{\alpha(\beta-1)}} \leq \gamma_{th}\right] \\
&= 1 - \mathcal{P}\Bigg[P_y.G_y.{d_y}^{\alpha(\beta-1)} \\
&\leq \gamma_{th}\Bigg(\sum_{x=1}^{M} P_x.G_x.{d_x}^{\alpha(\beta-1)} \\
&+ \sum_{\substack{z=1 \\ z\neq y}}^{L} P_z.G_z.{d_z}^{\alpha(\beta-1)}\Bigg)\Bigg] \\
&= 1 - \mathcal{P}\Bigg[G_y \leq \gamma_{th} \\
&\times {P_y}^{-1}{d_y}^{\alpha(1-\beta)}.\Bigg(\sum_{x=1}^{M} P_x.G_x.{d_x}^{\alpha(\beta-1)} \\
&+ \sum_{\substack{z=1 \\ z\neq y}}^{L} P_z.G_z.{d_z}^{\alpha(\beta-1)}\Bigg)\Bigg] \\
&= 1 - E\Bigg[exp\Bigg(-\gamma_{th}(P_y)^{-1}{d_y}^{\alpha(1-\beta)} \\
&\times \Bigg(\sum_{x=1}^{M} P_x.G_x.{d_x}^{\alpha(\beta-1)} \\
&+ \sum_{\substack{z=1 \\ z\neq y}}^{L} P_z.G_z.{d_z}^{\alpha(\beta-1)}\Bigg)\Bigg)\Bigg] \\
&= 1 - E_{(P_y)^{-1}{d_y}^{\alpha(1-\beta)}}\Big[\mathcal{L}_{I_c}(s) \times \mathcal{L}_{I_{d_i}}(s)\Big]
\end{aligned}
\tag{41}
$$

where E and s denotes the expectation operator and the Laplace domain variable.
Similarly, the coverage probability of D2D in the outer mode may be expressed as,

$$
\begin{aligned}
\mathcal{P}[\gamma_{d_o} \geq \gamma_{th}] &= 1 - E\Bigg[exp\Bigg(-\gamma_{th} \\
&\times (P_k)^{-1}{d_y}^{\alpha(1-\beta)} \sum_{\substack{z=1 \\ z\neq y}}^{L} P_z.G_z.{d_z}^{\alpha(\beta-1)}\Bigg)\Bigg] \\
&= 1 - E_{(P_k)^{-1}{d_y}^{\alpha(1-\beta)}}\Big[\mathcal{L}_{I_{d_o}}(s)\Big]
\end{aligned}
\tag{42}
$$

Here, $I_c = \sum_{x=1}^{M} P_x.G_x.{d_x}^{\alpha(\beta-1)}$ and $I_{d_i} = \left(\sum_{\substack{z=1 \\ z\neq y}}^{L} P_z.G_z.{d_z}^{\alpha(\beta-1)}\right)$ which signifies the interference of CU and inner mode D2Ds, respectively. However, from the definition it is clear that the Laplace transform of the interference is the exponential expectation of all of the interferences (I) i.e.,

$$
L_I(s) = E_I[e^{-sI}] \tag{43}
$$

Applying Laplace transform to the interference at D2Ds in inner mode, we get,

$$
\begin{aligned}
&\mathcal{L}_{I_{d_i}}(s) \\
&= E\Bigg[exp\Bigg(-s\Bigg(\sum_{\substack{z=1 \\ z\neq y}}^{L} P_z.G_z.{d_z}^{\alpha(\beta-1)}\Bigg)\Bigg)\Bigg] \\
&= E\Bigg[\prod_{z\in\phi} \frac{1}{1 + sP_z{d_z}^{-\alpha(1-\beta)}}\Bigg] \\
&= exp\Bigg(-\rho_{d_i}\int_0^{\infty}\Bigg(2\pi q\Bigg(1 - \frac{1}{1 + sP_z q^{-\alpha(1-\beta)}}\Bigg)\Bigg)dq\Bigg) \\
&= exp\Bigg(-\pi(sP_z)^{\tau}\rho_{d_i}\int_0^{\infty}\Bigg(\frac{1}{1 + sP_z q^{-\tau}}\Bigg)dq\Bigg) \\
&= exp\Bigg(-\pi(sP_z)^{\tau}\rho_{d_i}\pi\tau.cosec(\pi\tau)\Bigg)
\end{aligned}
\tag{44}
$$

where $\tau = \frac{2}{\alpha(1-\beta)}$
Similarly, applying the Laplace transform to interference at CUs, we get,

$$\begin{aligned}
&\mathcal{L}_{I_c}(s) \\
&= E\left[exp\left(-s\left(\sum_{x=1}^{M} P_x G_x {d_x}^{\alpha(\beta-1)}\right)\right)\right] \\
&= E\left[\prod_{x\in\phi} \frac{1}{1+sP_x {d_x}^{-\alpha(1-\beta)}}\right] \\
&= exp\left(-\pi(sP_x)^{\tau}\rho_c \pi\tau cosec(\pi\tau)\right)
\end{aligned} \tag{45}$$

Again, the interference of the D2Ds in the outer mode may be transformed using the Laplace transform,

$$\begin{aligned}
&\mathcal{L}_{I_{d_o}}(s) \\
&= E\left[exp\left(-s\left(\sum_{\substack{z=1 \\ z\neq k}}^{L} P_z G_z {d_z}^{\alpha(\beta-1)}\right)\right)\right] \\
&= exp\left(-\pi(sP_k)^{\tau}\rho_{d_o} \pi\tau cosec(\pi\tau)\right)
\end{aligned} \tag{46}$$

On substituting these values from equations (44) and (46) in equation (41), we get,

$$\begin{aligned}
P_{cov}^{d} = 1 - exp&\left(-\pi(sP_z)^{\tau}\rho_{d_i} \pi\tau cosec(\pi\tau)\right) \\
&\times exp\left(-\pi(sP_x)^{\tau}\rho_c \pi\tau cosec(\pi\tau)\right)
\end{aligned} \tag{47}$$

where ρ_c, ρ_{d_i} and ρ_{d_o} are the densities of CUs, D2Ds in inner mode, and D2Ds in outer mode, respectively.

4 Simulation results

In the proposed system, we consider a single cell scenario in which BS is located at focal point, while CUs and D2Ds follows PPP distribution within the cell. The different parameters considered for the simulations are as follows: the radius of cell is 500 m, the bandwidth used in the simulation is 1 GHz. In our work, we have limited the number of CUs to 100. It is assumed that the distance between D2Ds is approximately 30 metres. Here, we have considered two operating frequencies namely, 2 GHz for D2Ds communicating in inner mode and 28 GHz for D2Ds communicating in outer mode. Focusing mainly on 3GPP (3^{rd} Generation Partnership Project) constraints, the path loss model for signal propagation is derived from equations 1 and 2 [27]. The path loss exponent (α) is considered to be in the range of 2 to 3.

Table 2 Simulation parameters

Sl.	Parameters	Values
1	Cell radius	500 m
2	Bandwidth	1 GHz
3	Operating frequency	2 GHz, 28 GHz
4	Thermal noise density	−174 dBm/ Hz
5	D2D SINR threshold	0 dBm
6	Cellular SINR threshold	0 dBm
7	Maximum D2D transmit power	15 dBm
8	Maximum Cellular transmit power	30 dBm

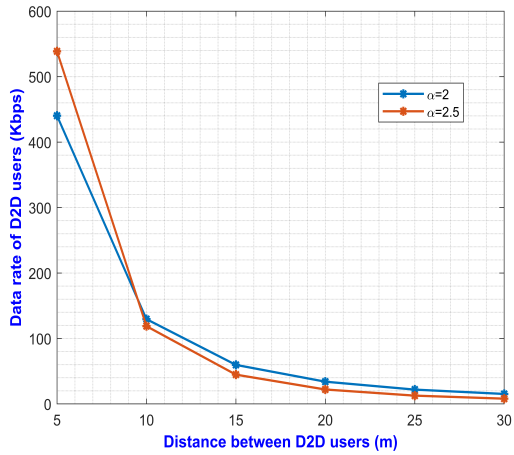

Fig. 2 Distance between D2D users vs data rate for varying pathloss exponents.

In Figure 2, as the path loss exponent value decreases from 2.5 to 2 at a distance of 5 m between the D2Ds, the data rate of the D2Ds also drop from 540 Kbps to 440 Kbps due to the adequate amount of interference present in the channel. At a distance of 10 m, the data rate of D2Ds is found to increase from 120 Kbps to 130 Kbps. Equations (8) and (11) give the relation between data rate of D2Ds and distance between

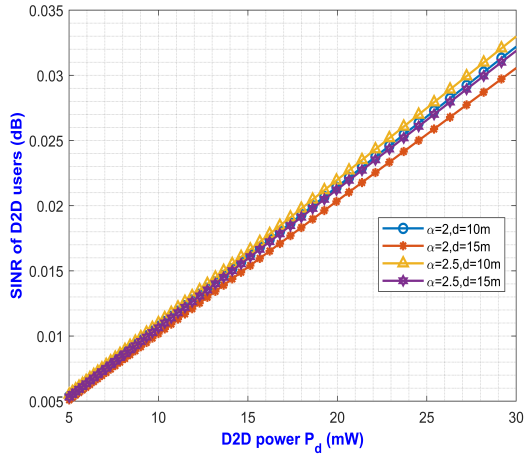

Fig. 3 SINR of D2D users vs D2D power for varying distance between D2D users and pathloss exponents.

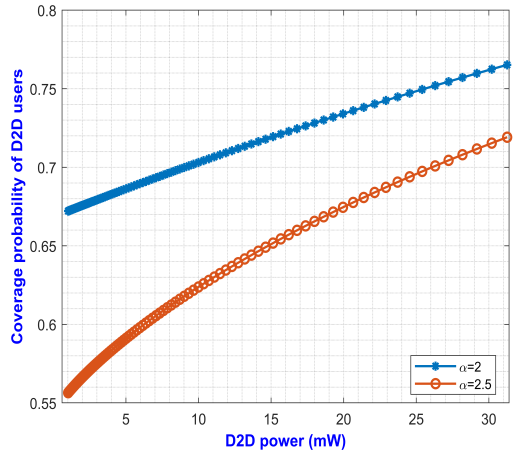

Fig. 4 Coverage probability of D2D users vs D2D power for varying pathloss exponents.

D2Ds. Thus, it is evident from the above equations that with a slight decrease in pathloss exponent from 2.5 to 2, there is an increase in data rate for varying distance between D2Ds from 10 to 20 m.

Figure 3 plots the D2D transmit power versus corresponding SINR for varying pathloss exponents and distance between D2Ds. With an increase in distance, SINR decreases therefore, throughput also decreases at a certain power. From equation (23), it can be noticed that with an increase in distance, SINR decreases substantially which results in the decrease of the data rate. For a given pathloss exponent of 2.5, the SINR for 30 mW D2D power declines from roughly 0.033 dB to around 0.032 dB as the distance increases from 10 to 15 m. As a result, it can be inferred from equation (38) that as the distance increases from 10 to 15 m, there is a drop in transmit power, but there is a minor change in SINR, i.e. about 0.001 dB, indicating that power is optimized efficiently. The plot gives an idea of the impact of the path loss exponent over D2D power in mW and its corresponding SINR values in decibel (dB).

The coverage probability is considered to be a prominent parameter for the system design. Figure 4 shows the graph for the D2D transmit power with respect to the coverage probability of D2D users. From equation (47), it can be inferred that for a small decrease in pathloss exponent there is also a decrease in D2D transmit power, resulting in a significant improvement in the coverage probability. Thus, the numerical results

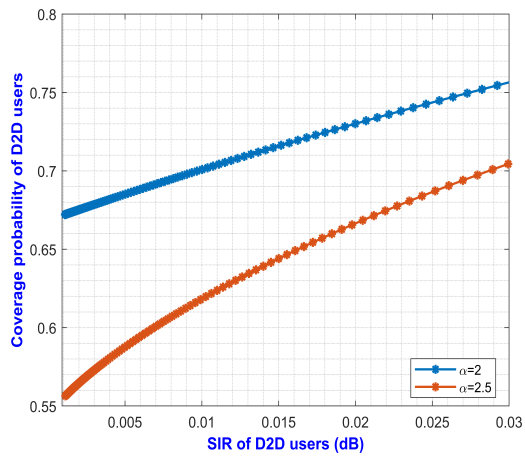

Fig. 5 Signal-to-Interference Ratio (SIR) vs coverage probability of D2D users for varying pathloss exponents.

indicate that for 15mW D2D transmit power at $\alpha = 2.5$, the coverage probability is about 0.71, whereas for the same D2D transmit power at $\alpha = 2$, the coverage probability improves to 0.77. As a result, decrease in pathloss exponent provides a higher probability of coverage. As a result, it can be noticed that the coverage probability varies dramatically for different pathloss exponent values. Thus, given a certain pathloss exponent, increasing the D2D transmit power from 10 mW to 30 mW results in a considerable improvement in coverage probability from 0.70 to 0.71. This indicates that increasing D2D transmit power has an affect on the QoS constraints. This motivates us

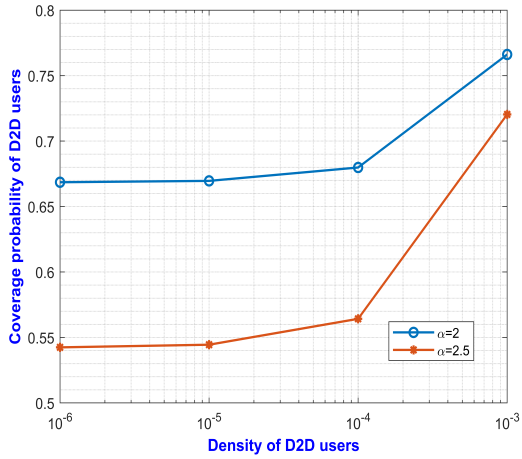

Fig. 6 Density vs coverage probability of D2D users for varying pathloss exponents.

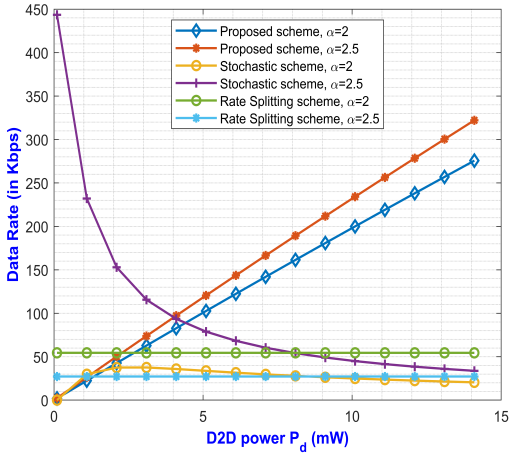

Fig. 7 Comparison of data rate for different schemes with varying pathloss exponents.

for finding the optimal D2D transmit power while satisfying the QoS constraints.

Figure 5 portrays the variation in Signal-to-Interference Ratio (SIR) of D2D users versus coverage probability for varying pathloss exponents. From equations (40) and (41), it can be inferred that with decrease in pathloss exponent, transmit power substantially increases which results in the increase of the coverage probability for a fixed SIR of D2Ds. Thus, we acquire a coverage probability of roughly 0.66 for $\alpha = 2.5$, and a coverage probability of 0.73 for $\alpha = 2$ with a fixed SIR of 0.02 dB for D2Ds. As a result, in an interference-limited environment, there is a little variation in the SIR of D2Ds ranging from 0.015 dB to 0.03 dB, but a large difference in the coverage probability ranging from 0.71 to 0.76.

In Figure 6, a graph is plotted between the density and the coverage probability of D2Ds. It is evident from the graph that the density of D2Ds varies from 10^{-6} to 10^{-3} per cubic meter. From equations (3) and (8), it can be inferred that when the density of D2Ds increases, the throughput of D2Ds decreases, and as a result, the coverage probability of the D2Ds reduces. Thus, with the increase in the density of the D2Ds, coverage probability of D2Ds also increases eventually. Because the pathloss exponent is so important, it is critical to determine the equivalent coverage probability for varied path loss models. At a density of 10^{-6}, the coverage probability of D2Ds declines from 0.67 to 0.54 as pathloss exponent increases from 2 to 2.5.

Finally, in Figure 7, the proposed scheme is compared with the stochastic scheme [28] and rate splitting scheme [29]. The transmit power of the D2D users are varied from 1 to 15 mW with varying pathloss exponents of 2 and 2.5. The stochastic scheme yields a data rate of around 450 Kbps at a pathloss exponent of 2.5. But there is an exponential decrease in the data rate which makes it unsuitable. While in the rate splitting scheme, the data rate is low but it is consistent for varying D2D transmit power. Whereas, in the proposed work, the data rate of the D2Ds for varying D2D transmit power and pathloss exponent gives better result when compared with the state-of-the-art schemes namely, stochastic and rate splitting. The weight attached to the D2D transmit power optimizes the power enhancing the overall D2D throughput. Thus, as evident from the figure, it can be inferred that the data rate achieved from the proposed scheme attains higher data rate of around 330 Kbps at a pathloss exponent of 2.5 in comparison to the state-of-the-art schemes.

4.1 Computational complexity

The computational complexity of the Algorithm 1 can be approximated by the three for loops from line 4 to line 21, line 5 to line 20 and line 6 to line 19, respectively. Also, the conditional statement $if - else$ is used in line 8 to line 16. Since, the cardinality of D2D and cellular users are L and N respectively, the computational complexity for the three for loops in worst case is $O(N \times (L -$

1)). Again, the time complexity of the $If - else$ statement can be given by $O(1)$. Thus, the computational complexity of the proposed scheme can be approximated by $O(N \times L) + O(n \times l \times f \mid J \mid)$. Here, $f \mid J \mid$ represents the computational complexity of the formulated problem as shown in equation (40). As we have considered a finite number of D2D pairs, it implies that the complexity of the second term is negligible and can be ignored. Thus, the computational complexity of Algorithm 1 is given by $O(N \times (L-1))$.

5 Conclusion and future scope

The paper analyzes the performance of D2D communication using dynamic mode selection in a mm-Wave network employing an uplink channel. D2D communication in mm-Wave networks has its own set of challenges to overcome. The mm-Wave frequency introduces a significant amount of interference, resulting in signal attenuation due to path loss. The proposed scheme describes two modes, inner mode and outer mode for the utilization of spectrum resources for D2D communication. The derived radius of coverage specifies the limit for switching of modes. If the radius of coverage is less than a certain value r, then the D2D user will operate in inner mode at a frequency of 2 GHz else it will operate in outer mode at a frequency of 28 GHz. The outer mode switching occurs when there is a substantial proportion of D2D users in close proximity with escalating path loss exponents. As a result, the suggested power optimization for each D2D user is conducted on the pre-assigned channels using the Lagrange dual optimization method in order to increase the data rate of D2D while minimizing their transmit power. As the number of users proliferates every day, the probability of coverage is enhanced while satisfying the QoS constraints. Furthermore, when the SINR of the D2Ds increase, the coverage probability of D2Ds also increases. The coverage probability of the proposed method assures higher performance, which undoubtedly allows D2D communication in a 5G mm-Wave network. Simulation results prove the effectiveness of the proposed methodology. Also, the proposed approach is compared with the existing techniques which further validates the efficiency. The future scope includes a scenario in which the BS has incomplete knowledge of the CSI for all network links. Because, in real-world circumstances, service providers may not be willing to share all CSI data for obvious monetary reasons. In future study, machine learning techniques can be applied to maximize throughput, SINR and coverage probability. The use of reinforcement learning and deep learning techniques may prove beneficial in obtaining better outcomes.

Declarations

- Funding: The authors declare that no funds, grants, or other support were received during the preparation of this manuscript.
- Competing interests: The authors have no relevant financial or non-financial interests to disclose.
- Data Availability: Data sharing not applicable to this article as no datasets were generated or analysed during the current study.
- Authors' contributions: All authors contributed equally to the study conception and design. System modelling and analysis were performed by Subhra Sankha Sarma, Atul Sachan, Ranjay Hazra and FA Talukdar. The first draft of the manuscript was written by Subhra Sankha Sarma and Atul Sachan. All the authors have read and approved the final manuscript.

References

1. Agiwal, M., Roy, A. and Saxena, N., 2016. Next generation 5G wireless networks: A comprehensive survey. IEEE Communications Surveys & Tutorials, 18(3), pp.1617-1655.
2. Asadi, A., Wang, Q. and Mancuso, V., 2014. A survey on device-to-device communication in cellular networks. IEEE Communications Surveys & Tutorials, 16(4), pp.1801-1819.
3. Liu, Z., Peng, T., Xiang, S. and Wang, W., 2012, June. Mode selection for device-to-device (D2D) communication under LTE-advanced networks. In 2012 IEEE International Conference on Communications (ICC) (pp. 5563-5567). IEEE.
4. Wei, L., Hu, R.Q., Qian, Y. and Wu, G., 2014. Enable device-to-device communications underlaying cellular networks: challenges and research aspects. IEEE Communications Magazine, 52(6), pp.90-96.

5. Gupta, A. and Jha, R.K., 2015. A survey of 5G network: Architecture and emerging technologies. IEEE access, 3, pp.1206-1232.
6. Sarma, S.S. and Hazra, R., 2020. Interference mitigation methods for D2D communication in 5G network. In Cognitive Informatics and Soft Computing (pp. 521-530). Springer, Singapore.
7. Waqas Haider Shah, S., Li, R., Mahboob Ur Rahman, M., Noor Mian, A., Aman, W. and Crowcroft, J., 2021. Statistical QoS guarantees of a device-to-device link assisted by a full-duplex relay. Transactions on Emerging Telecommunications Technologies, 32(11), p.e4339.
8. Soultan, E.M., Nafea, H.B. and Zaki, F.W., 2021. Interference management for different 5G cellular network constructions. Wireless personal communications, 116(3), pp.2465-2484.
9. Bany Salameh, H., Al-Bzoor, R. and Darabkh, K.A., 2022. Exploiting device-to-device (D2D) transmission strategy for throughput enhancement in WLANs. Wireless Networks, pp.1-11.
10. Rappaport, T.S., Sun, S., Mayzus, R., Zhao, H., Azar, Y., Wang, K., Wong, G.N., Schulz, J.K., Samimi, M. and Gutierrez, F., 2013. Millimeter wave mobile communications for 5G cellular: It will work!. IEEE access, 1, pp.335-349.
11. Yağcıoğlu, M., Dynamic resource allocation and interference coordination for millimeter wave communications in dense urban environment. Transactions on Emerging Telecommunications Technologies, p.e4442.
12. Feng, D., Yu, G., Xiong, C., Yuan-Wu, Y., Li, G.Y., Feng, G. and Li, S., 2015. Mode switching for energy-efficient device-to-device communications in cellular networks. IEEE Transactions on Wireless Communications, 14(12), pp.6993-7003.
13. Huang, Y., Nasir, A.A., Durrani, S. and Zhou, X., 2016. Mode selection, resource allocation, and power control for D2D-enabled two-tier cellular network. IEEE Transactions on communications, 64(8), pp.3534-3547.
14. Khuntia, P. and Hazra, R., 2021. An Efficient Channel and Power Allocation Scheme for D2D Enabled Cellular Communication System: An IoT Application. IEEE Sensors Journal.
15. Yu, C.H., Tirkkonen, O., Doppler, K. and Ribeiro, C., 2009, June. Power optimization of device-to-device communication underlaying cellular communication. In 2009 IEEE international conference on communications (pp. 1-5). IEEE.
16. Lee, N., Lin, X., Andrews, J.G. and Heath, R.W., 2014. Power control for D2D underlaid cellular networks: Modeling, algorithms, and analysis. IEEE Journal on Selected Areas in Communications, 33(1), pp.1-13.
17. Venugopal, K., Valenti, M.C. and Heath, R.W., 2016. Device-to-device millimeter wave communications: Interference, coverage, rate, and finite topologies. IEEE Transactions on Wireless Communications, 15(9), pp.6175-6188.
18. Sarma, S.S., Khuntia, P. and Hazra, R. Power control scheme for device-to-device communication using uplink channel in 5G mm-Wave network. Transactions on Emerging Telecommunications Technologies, vol. 33, issue 6, 2022.
19. Qiao, J., Shen, X.S., Mark, J.W., Shen, Q., He, Y. and Lei, L., 2015. Enabling device-to-device communications in millimeter-wave 5G cellular networks. IEEE Communications Magazine, 53(1), pp.209-215.
20. Sarma, S.S. and Hazra, R., 2020, February. Interference management for D2D communication in mm-Wave 5G network: An Alternate Offer Bargaining Game theory approach. In 2020 7th International Conference on Signal Processing and Integrated Networks (SPIN) (pp. 202-207). IEEE.
21. Zhong, B., Zhang, J., Zeng, Q. and Dai, X., 2016. Coverage probability analysis for full-duplex relay aided device-to-device communications networks. China Communications, 13(11), pp.60-67.
22. Bai, T. and Heath, R.W., 2014. Coverage and rate analysis for millimeter-wave cellular networks. IEEE Transactions on Wireless Communications, 14(2), pp.1100-1114.
23. Sarma, S.S., Harza, R., and Mukherjee, A., "Symbiosis between D2D communication and Industrial IoT for Industry 5.0 in 5G mm-Wave cellular network: An interference management approach," in IEEE Transactions on Industrial Informatics, vol. 18, no. 8, pp. 5527-5536, 2022.
24. Singh, I. and Singh, N.P., 2018. Coverage and capacity analysis of relay-based device-to-device communications underlaid cellular networks. Engineering Science and Technology, an International Journal, 21(5), pp.834-842.

25. Sun, S., MacCartney, G.R. and Rappaport, T.S., 2017, May. A novel millimeter-wave channel simulator and applications for 5G wireless communications. In 2017 IEEE International Conference on Communications (ICC) (pp. 1-7). IEEE.
26. Ju, S., Kanhere, O., Xing, Y. and Rappaport, T.S., 2019, December. A millimeter-wave channel simulator NYUSIM with spatial consistency and human blockage. In 2019 IEEE Global Communications Conference (GLOBECOM) (pp. 1-6). IEEE.
27. Ghosh, A., Maeder, A., Baker, M. and Chandramouli, D., 2019. 5G evolution: A view on 5G cellular technology beyond 3GPP release 15. IEEE access, 7, pp.127639-127651.
28. Song, X.A., Li, H., Guo, Z. and Wang, X.P., 2019, July. Coverage Probability Analysis of D2D Communication Based on Stochastic Geometry Model. In International Conference in Communications, Signal Processing, and Systems (pp. 83-93). Springer, Singapore.
29. Yang, Z., Chen, M., Saad, W., Xu, W. and Shikh-Bahaei, M. Sum-rate maximization of uplink rate splitting multiple access (RSMA) communication. IEEE Transactions on Mobile Computing, vol. 21, no. 7, pp. 2596-2609, 2022.